NASA TN D-1156

TECHNICAL NOTE

D-1156

THEORETICAL FLUTTER ANALYSIS OF FLAT RECTANGULAR PANELS IN UNIFORM COPLANAR FLOW WITH ARBITRARY DIRECTION

By Eldon E. Kordes and Richard B. Noll

Flight Research Center
Edwards, Calif.

NATIONAL AERONAUTICS AND SPACE ADMINISTRATION

WASHINGTON

January 1962

NATIONAL AERONAUTICS AND SPACE ADMINISTRATION

TECHNICAL NOTE D-1156

THEORETICAL FLUTTER ANALYSIS OF FLAT RECTANGULAR PANELS IN UNIFORM COPLANAR FLOW WITH ARBITRARY DIRECTION

By Eldon E. Kordes and Richard B. Noll

SUMMARY

A theoretical analysis is presented of the flutter of simply supported flat rectangular panels in uniform coplanar flow with arbitrary direction. The results of numerical calculations are included for flow angles between 0° and 90° and for values of length-width ratio squared between 0.2 and 5.0. These results showed that the critical flutter mode changes at small flow angles for panels with length-width ratios less than 1.

Changes in flow direction were shown to have a marked effect on the critical dynamic-pressure parameter. This effect was most pronounced for panels with small values of length-width ratio, and the flutter of panels becomes less susceptible to small variations in flow angle as the length-width ratio becomes larger.

The flutter condition of identical panels at different flow angles was compared on a common basis by utilizing curves which present the ratio of critical dynamic-pressure parameter at any flow angle to the critical dynamic-pressure parameter at a predetermined flow angle as a function of flow direction.

INTRODUCTION

The flutter of skin panels on the exposed surfaces of supersonic vehicles has been the subject of many theoretical and experimental investigations. The results of these investigations are summarized and discussed in reference 1. More recently, additional research information has been published on the flutter of flat panels (see, for example, refs. 2 to 6). With the exception of a limited treatment in reference 6, none of the papers on the flutter of flat rectangular panels has included results for flow direction other than parallel to

one side of the panel. Since panel orientation and vehicle maneuvers during flight subject exposed skin panels to many different flow directions, it is important to investigate the effect of flow angle on panel flutter.

In order to assess the importance of the flow angle on panel flutter, a theoretical analysis is presented for the flutter of simply supported rectangular panels in uniform coplanar flow with arbitrary direction; that is, the direction of flow is not restricted to be parallel with a side of the panel. Results of numerical calculations based on a modal analysis and linearized, two-dimensional aerodynamics are included for flow angles between 0° and 90° over flat panels with values of $(l/w)^2$ between 0.2 and 5.0.

SYMBOLS

$A = -2\pi^2\left(\frac{l}{w}\right)^2$

$\overline{A},\overline{B},\overline{C}$	coefficients defined by equations (10), (11), and (12), respectively
B_n	frequency parameter, $k^2 - (n\pi)^4\left(\frac{l}{w}\right)^4$
C_{mn}	Fourier series coefficients
D	flexural rigidity of isotropic plate, $\frac{Et^3}{12\left(1 - \nu^2\right)}$
E	Young's modulus of elasticity
h,j,m,n,r,s	integers
$i = \sqrt{-1}$	
k	frequency coefficient, $\omega l^2\sqrt{\frac{\gamma}{D}}$
$L(x,y,\tau)$	lateral aerodynamic loading
$\overline{L}_{mn,rs}$	generalized force coefficient defined by equation (6)
l	panel length
M	Mach number
$\overline{P}_{mn,rs}$	generalized force coefficient defined by equation (6)
q	dynamic pressure, $\frac{\rho V^2}{2}$

Re	real part
S	coordinate in direction of flow
t	panel thickness
V	flow velocity
$W(x,y,\tau)$	lateral deflection of panel
w	panel width
x,y	Cartesian coordinates
$\beta = \sqrt{M^2 - 1}$	
γ	mass per unit area of panel
Λ	flow angle in the plane of the panel, deg
λ	dynamic-pressure parameter, $\frac{2ql^3}{\beta D}$
λ_{cr}	critical dynamic-pressure parameter
$\left(\lambda_{cr}\right)_\Lambda$	critical dynamic-pressure parameter at the indicated flow angle
ν	Poisson's ratio
ρ	mass density of air
τ	time
ω	circular frequency

$$\nabla^4 = \frac{\partial^4}{\partial x^4} + 2\frac{\partial^4}{\partial x^2 \partial y^2} + \frac{\partial^4}{\partial y^4}$$

Subscripts:

m,n,r,s	integers
x,y,τ	denotes differentiation with respect to indicated variable

ANALYSIS

An analysis is presented of the flutter of flat, rectangular panels with supersonic flow over one surface where the flow direction is arbitrary in the plane of the panel; that is, the flow is not restricted to a direction parallel to a side of the panel. The analysis is based on small-deflection thin-plate theory for isotropic plates without midplane stresses (see ref. 7).

The panel geometry and coordinate system used in the analysis are shown in figure 1. The x-y plane defines the middle plane of a uniform thickness plate before loading, and the x-axis coincides with one edge of the plate. The plate is assumed to have thickness t, length l in the x-direction, and width w in the y-direction. Supersonic flow over one surface is assumed to form an angle Λ with the negative x-axis.

The equilibrium equation for a laterally loaded plate in the absence of midplane forces is

$$D\nabla^4 W + \gamma W_{\tau\tau} = L(x,y,\tau) \tag{1}$$

where $W(x,y,\tau)$ is the lateral deflection of the panel, D is the flexural rigidity, γ is the mass per unit area, and $L(x,y,\tau)$ is the lateral loading per unit area. In equation (1) the subscripts represent differentiation with respect to the indicated variable.

It is assumed that Ackeret's theory of linearized, two-dimensional supersonic aerodynamic loading gives an adequate approximation to the air forces for high Mach numbers. For a flow at an angle Λ the aerodynamic load per unit area is given by

$$L(x,y,\tau) = \frac{-2q}{\beta}\frac{dW}{dS} = \frac{-2q}{\beta}\left(W_x \cos\Lambda + W_y \sin\Lambda\right) \tag{2}$$

where q is the dynamic pressure $\frac{\rho V^2}{2}$, $\beta = \sqrt{M^2 - 1}$, and M is the Mach number.

For a simply supported panel, the boundary conditions are

$$\left.\begin{aligned} W(0,y,\tau) &= W(l,y,\tau) = 0 \\ W(x,0,\tau) &= W(x,w,\tau) = 0 \\ W_{xx}(0,y,\tau) &= W_{xx}(l,y,\tau) = 0 \\ W_{yy}(x,0,\tau) &= W_{yy}(x,w,\tau) = 0 \end{aligned}\right\} \tag{3}$$

and the lateral deflection which satisfies equation (3) can be written in the form

$$W(x,y,\tau) = \mathrm{Re}\left(\sum_m \sum_n C_{mn} \sin \frac{m\pi x}{l} \sin \frac{n\pi y}{w} e^{i\omega\tau}\right) \tag{4}$$

where ω is the circular frequency. In general ω is complex; however, for simple harmonic motion ω must be real.

H 2 6 5

Substituting equation (4) into equation (1), multiplying by $\sin \frac{r\pi x}{l} \sin \frac{s\pi y}{w}$, and integrating yields the following set of equations for the coefficients C_{mn}

$$\left[(m\pi)^4 - (mn\pi)^2 A - B_n\right] C_{mn} + \lambda \cos \Lambda \sum_{r=1}^{h} \sum_{s=1}^{j} \bar{L}_{mn,rs} C_{rn} + \lambda \frac{l}{w} \sin \Lambda \sum_{r=1}^{h} \sum_{s=1}^{j} \bar{P}_{mn,rs} C_{ns} = 0 \tag{5}$$

where

$$\left.\begin{aligned}
&\bar{L}_{mn,rs} = \frac{4mr}{m^2 - r^2}; \quad n = s, \quad m + r \text{ odd} \\
&\bar{L}_{mn,rs} = 0; \quad n = s, \quad m + r \text{ even} \\
&\bar{L}_{mn,rs} = 0; \quad n \neq s \\
&\bar{P}_{mn,rs} = \frac{4ns}{n^2 - s^2}; \quad m = r, \quad n + s \text{ odd} \\
&\bar{P}_{mn,rs} = 0; \quad m = r, \quad n + s \text{ even} \\
&\bar{P}_{mn,rs} = 0; \quad m \neq r
\end{aligned}\right\} \tag{6}$$

and

$$\left.\begin{aligned}
A &= -2\pi^2 \left(\frac{l}{w}\right)^2 \\
B_n &= k^2 - (n\pi)^4 \left(\frac{l}{w}\right)^4 \\
\lambda &= \frac{2ql^3}{\beta D} \\
k^2 &= \frac{\gamma l^4}{D} \omega^2
\end{aligned}\right\} \tag{7}$$

Equation (5), together with equation (4), defines the deflectional behavior of a simply supported panel in the presence of supersonic flow over one surface at an arbitrary flow angle Λ. If Λ is assigned the value of zero in equation (5), the resulting relation agrees with the results of the Galerkin solution presented in reference 8 for the condition of no midplane stresses.

For a nontrivial solution, the determinant of coefficients of C_{mn} must equal zero. If the analysis is limited to two modes in both the x- and y-directions, for example, $h = 2$, $j = 2$, the determinant becomes

$$\begin{vmatrix} \pi^4 - \pi^2 A - B_1 & -\frac{8}{3}\lambda\cos\Lambda & -\frac{8}{3}\frac{l}{w}\lambda\sin\Lambda & 0 \\ \frac{8}{3}\lambda\cos\Lambda & 16\pi^4 - 4\pi^2 A - B_1 & 0 & -\frac{8}{3}\frac{l}{w}\lambda\sin\Lambda \\ \frac{8}{3}\frac{l}{w}\lambda\sin\Lambda & 0 & \pi^4 - 4\pi^2 A + 15\pi^4\left(\frac{l}{w}\right)^4 - B_1 & -\frac{8}{3}\lambda\cos\Lambda \\ 0 & \frac{8}{3}\frac{l}{w}\lambda\sin\Lambda & \frac{8}{3}\lambda\cos\Lambda & 16\pi^4 - 16\pi^2 A + 15\pi^4\left(\frac{l}{w}\right)^4 - B_1 \end{vmatrix} = 0 \tag{8}$$

where B_n has been replaced by $B_n = B_1 - \left(n^4 - 1\right)\left(\frac{l}{w}\right)^4\pi^4$.

By expanding equation (8) and solving for λ, the following relation is obtained

$$\overline{A}^2\lambda^4 + \overline{B}\lambda^2 + \overline{C} = 0 \tag{9}$$

where

$$\overline{A} = \left(\frac{8}{3}\cos\Lambda\right)^2 - \left(\frac{8}{3}\frac{l}{w}\sin\Lambda\right)^2 \tag{10}$$

$$\overline{B} = \left\{\pi^8\left[257 + 650\left(\frac{l}{w}\right)^2 + 527\left(\frac{l}{w}\right)^4 + 150\left(\frac{l}{w}\right)^6\right] - \pi^4 B_1\left[34 + 50\left(\frac{l}{w}\right)^2 + 30\left(\frac{l}{w}\right)^4\right] + 2B_1^2\right\}\left(\frac{8}{3}\frac{l}{w}\sin\Lambda\right)^2 + \left\{\pi^8\left[32 + 200\left(\frac{l}{w}\right)^2 + 527\left(\frac{l}{w}\right)^4 + 600\left(\frac{l}{w}\right)^6 + 225\left(\frac{l}{w}\right)^8\right] - \pi^4 B_1\left[34 + 50\left(\frac{l}{w}\right)^2 + 30\left(\frac{l}{w}\right)^4\right] + 2B_1^2\right\}\left(\frac{8}{3}\cos\Lambda\right)^2 \tag{11}$$

$$\overline{C} = \left\{\pi^8\left[16 + 40\left(\frac{l}{w}\right)^2 + 16\left(\frac{l}{w}\right)^4\right] - \pi^4 B_1\left[17 + 10\left(\frac{l}{w}\right)^2\right] + B_1^2\right\}\left\{\pi^8\left[16 + 160\left(\frac{l}{w}\right)^2 + 511\left(\frac{l}{w}\right)^4 + 600\left(\frac{l}{w}\right)^6 + 225\left(\frac{l}{w}\right)^8\right] - \pi^4 B_1\left[17 + 40\left(\frac{l}{w}\right)^2 + 30\left(\frac{l}{w}\right)^4\right] + B_1^2\right\} \tag{12}$$

Equation (9) is used to obtain critical values of λ for which one of the eigenvalues κ^2 becomes complex and the panel becomes unstable. Where the flow direction is along a diagonal of the panel

$$\tan \Lambda = \frac{w}{l} \tag{13}$$

and $\overline{A}$ is zero. For this case the critical value of λ is determined from

$$\lambda^2 = -\frac{\overline{C}}{\overline{B}} \tag{14}$$

Once the critical value of λ is obtained, the form of the flutter mode can be obtained by solving equation (5) for the ratio of coefficients. Then the lateral deflection of the panel can be calculated from equation (4).

RESULTS AND DISCUSSION

The effect of the flow angle Λ on the flutter behavior of rectangular panels is illustrated in figure 2, where the dynamic-pressure parameter λ is shown as a function of the frequency parameter B_1. The results in figures 2(a) to 2(c) are for a panel with $\left(\frac{l}{w}\right)^2 = 0.3$ at $\Lambda = 0°$, 5°, and 10°, respectively, and were obtained from numerical solutions of equation (9). For $\lambda = 0$, the values of B_1 are real and can be shown to correspond to the first four natural frequencies of the plate in a vacuum, as indicated by the C_{mn} coefficients in figure 2. As λ increases, the values of B_1 change smoothly until a critical value of λ is reached where two values of B_1 become equal. A further increase in λ results in two complex

values of B_1, and the panel has an unstable mode of oscillation. The critical value of λ (see ref. 8) is described by the condition

$$\frac{\partial \lambda}{\partial B_1} = 0$$

It can be seen in figure 2(a) that for $\Lambda = 0°$ a condition exists where, for a value of λ less than λ_{cr}, two values of B_1 become equal; however, for this condition the values of B_1 are real and the motion remains stable with a further increase in λ.

The calculated results in figure 2 show that the principal effect of Λ is to change the critical flutter mode. This change in flutter mode can be seen by comparing figure 2(a) for $\Lambda = 0°$ with figure 2(b) for $\Lambda = 5°$. The nature of the mode change is clearly shown in figures 3(a) to 3(c), in which the calculated lateral-deflection shapes are shown for the critical flutter conditions in figure 2. In figure 3 the dashed line is used to represent the deflections in the opposite direction to the deflections shown by the solid curve. For $\Lambda = 0°$ (fig. 2(a)) the values of B_1 that coalesce correspond to the plate modes associated with C_{11} and C_{21}. The resulting flutter mode (fig. 3(a)) is composed of only these two plate modes (see eq. (4)). For $\Lambda = 5°$ and $\Lambda = 10°$ (figs. 2(b) and 2(c)) the values of B_1 that coalesce correspond to plate modes associated with C_{11} and C_{12}. The flutter modes for these flow angles are composed of all four of the assumed plate modes, as seen in figures 3(b) and 3(c). The change in the flutter mode is to be expected, inasmuch as for $\Lambda = 90°$ the flow direction is parallel to the long side of the panel and the calculated flutter mode is associated with the plate modes corresponding to C_{11} and C_{12}. The interesting feature shown in figure 3 is that the change in the flutter mode occurs for very small values of Λ; in fact, the calculations made during this investigation showed that for panels with $\frac{l}{w} < 1$ the mode change occurred for $\Lambda < 1°$.

The variation of the critical dynamic-pressure parameter λ_{cr} with flow angle Λ is shown in figure 4 for a panel with $\left(\frac{l}{w}\right)^2 = 0.3$. The results in figure 4 are based on λ in terms of l corresponding to the original flow direction $\Lambda = 0°$. The results show that λ_{cr} decreases rapidly with increasing flow angle. The sudden drop in the value of λ_{cr}, indicated by the dashed line, for a change in flow

direction from $\Lambda = 0°$ to $\Lambda = 0.5°$ is of interest. These results show that for a panel in supersonic flow at constant Mach number with the length-width ratio considered, the critical flutter speed predicted on the basis of $\Lambda = 0°$ would be unconservative if the panel is subjected to variations in flow direction. For example, a flow angle of $5°$ produces a 5.2-percent decrease in the value of λ_{cr} and a 2.6-percent decrease in the critical flutter speed predicted at $\Lambda = 0°$.

The change in λ_{cr} with length-width ratio is shown in figure 5 for several values of the flow angle. The results are for values of $\left(\frac{l}{w}\right)^2$ between 0.2 and 1.0. The effect of the flow direction on the critical value of the dynamic-pressure parameter is most pronounced for panels with small values of $\left(\frac{l}{w}\right)^2$. For values of $\left(\frac{l}{w}\right)^2$ near 0.2, the calculated values of λ_{cr} show a marked decrease with increases in flow angle. For panels with $\left(\frac{l}{w}\right)^2$ near 1.0, changes in the flow direction have a relatively minor effect on the critical values of the dynamic-pressure parameter; in fact, a small increase in flow angle from $\Lambda = 0°$ results in an increase in the value of λ_{cr}. These results show that small flow angles produce a slight stabilizing effect on panels with $\left(\frac{l}{w}\right)^2$ near 1.0 and a destabilizing effect on panels with $\left(\frac{l}{w}\right)^2$ near 0.2. The result in figure 5 indicates that considerable scatter in experimental panel-flutter data, for panels with $\frac{l}{w} < 1$, could be expected if the flow direction is not known accurately or varies during the test. Although the results are shown for $\left(\frac{l}{w}\right)^2 \leq 1$, the values of λ_{cr} for $\left(\frac{l}{w}\right)^2 > 1$ can be obtained from these curves by replacing l with w in the expression for the dynamic-pressure parameter (see eq. (7)) and taking into consideration the proper flow angle (complementary angles are used when l and w are interchanged).

The results of the calculations for several panels with length-width ratios in the range $0.2 \leq \left(\frac{l}{w}\right)^2 \leq 5$ are presented in figure 6. In this figure, the dynamic-pressure parameter is presented as the ratio $\frac{\left(\lambda_{cr}\right)_\Lambda}{\left(\lambda_{cr}\right)_{\Lambda = 0°}}$ so that all of the results can be compared on a common

basis. For the results shown, the critical dynamic-pressure parameter λ_{cr} changes smoothly as the flow angle Λ increases from 0° to 90° for all panels with $0.4 \leq \left(\frac{l}{w}\right)^2 \leq 2.0$. For panels with $\left(\frac{l}{w}\right)^2 < 0.4$, λ_{cr} changes suddenly for a flow angle slightly greater than zero; whereas, the sudden change in λ_{cr} occurs near $\Lambda = 90°$ for panels with $\left(\frac{l}{w}\right)^2 \geq 3.0$. The values of $\left(\frac{l}{w}\right)^2$ for which the sudden change in λ_{cr} occurs were not determined exactly; however, the results show that the change occurs for $0.3 < \left(\frac{l}{w}\right)^2 < 0.4$ and for $2.5 < \left(\frac{l}{w}\right)^2 < 3.0$. The abrupt changes in λ_{cr} near $\Lambda = 0°$ and 90° are indicated by the dashed lines.

H
2
6
5

Curves of the type shown in figure 6 can be used to obtain the critical dynamic-pressure parameter at various flow angles for a given panel if the flutter conditions are known at $\Lambda = 0°$, or the procedure can be reversed to find λ_{cr} at $\Lambda = 0°$ from known conditions at other flow angles. This latter procedure was used in reference 6 in an attempt to reduce flight flutter data for swept panels for comparison with wind-tunnel results obtained for a flow angle as near zero as practical. This comparison was not conclusive, since it was necessary to use the geometric angle of sweep and free-stream-flow conditions rather than the unknown local-flow angle and conditions. However, the data reduced by this procedure agreed more closely with the wind-tunnel results than if the effect of flow angle were neglected.

CONCLUSIONS

A theoretical analysis has been presented of the flutter of flat rectangular panels with an arbitrary flow direction in the plane of the panel. Calculated results are used to show that a variation in flow direction from parallel to one side of the panel to an arbitrary flow angle over the panel changes the critical flutter mode. This change in flutter characteristic occurred at small flow angles for panels with length-width ratios less than 1.

The critical dynamic-pressure parameter was shown to be affected also by further changes in flow direction following the mode change. This effect was most pronounced for panels with small values of length-width ratios, and the flutter of panels becomes less susceptible to small variations in flow angle as the panel length-width ratio becomes larger. Also, it was shown that variations from the desired flow angle in experimental tests can be expected to cause discrepancies in the flutter data.

The flutter condition of identical panels at different flow angles can be compared on a common basis by utilizing curves which present the ratio of critical dynamic-pressure parameter at any flow angle to the critical dynamic-pressure parameter at a predetermined flow angle as a function of flow direction.

Flight Research Center,
National Aeronautics and Space Administration,
Edwards, Calif., October 19, 1961

REFERENCES

1. Fung, Y. C. B.: A Summary of the Theories and Experiments on Panel Flutter. AFOSR TN 60-224, Guggenheim Aero. Lab., Calif. Inst. of Tech., May 1960.

2. Kordes, Eldon E., Tuovila, Weimer J., and Guy, Lawrence D.: Flutter Research on Skin Panels. NASA TN D-451, 1960.

3. Lock, M. H., and Fung, Y. C.: Comparative Experimental and Theoretical Studies of the Flutter of Flat Panels in a Low Supersonic Flow. AFOSR TN 670, Guggenheim Aero. Lab., Calif. Inst. of Tech., May 1961.

4. Tuovila, W. J., and Presnell, John G., Jr.: Supersonic Panel Flutter Test Results for Flat Fiber-Glass Sandwich Panels With Foamed Cores. NASA TN D-827, 1961.

5. Dixon, Sidney C., Griffith, George E., and Bohon, Herman L.: Experimental Investigation at Mach Number 3.0 of the Effects of Thermal Stress and Buckling on the Flutter of Four-Bay Aluminum Alloy Panels With Length-Width Ratios of 10. NASA TN D-921, 1961.

6. Kordes, Eldon E., and Noll, Richard B.: Flight Flutter Results for Flat Rectangular Panels. Presented at American Rocket Society Conference on Lifting Reentry Vehicles: Structures, Materials, and Design, Palm Springs, Calif., Apr. 4-7, 1961.

7. Timoshenko, S.: Theory of Plates and Shells. McGraw-Hill Book Co., Inc., 1940, ch. 4.

8. Hedgepeth, John M.: Flutter of Rectangular Simply Supported Panels at High Supersonic Speeds. Jour. Aero. Sci., vol. 24, no. 8, Aug. 1957, pp. 563-573, 586.

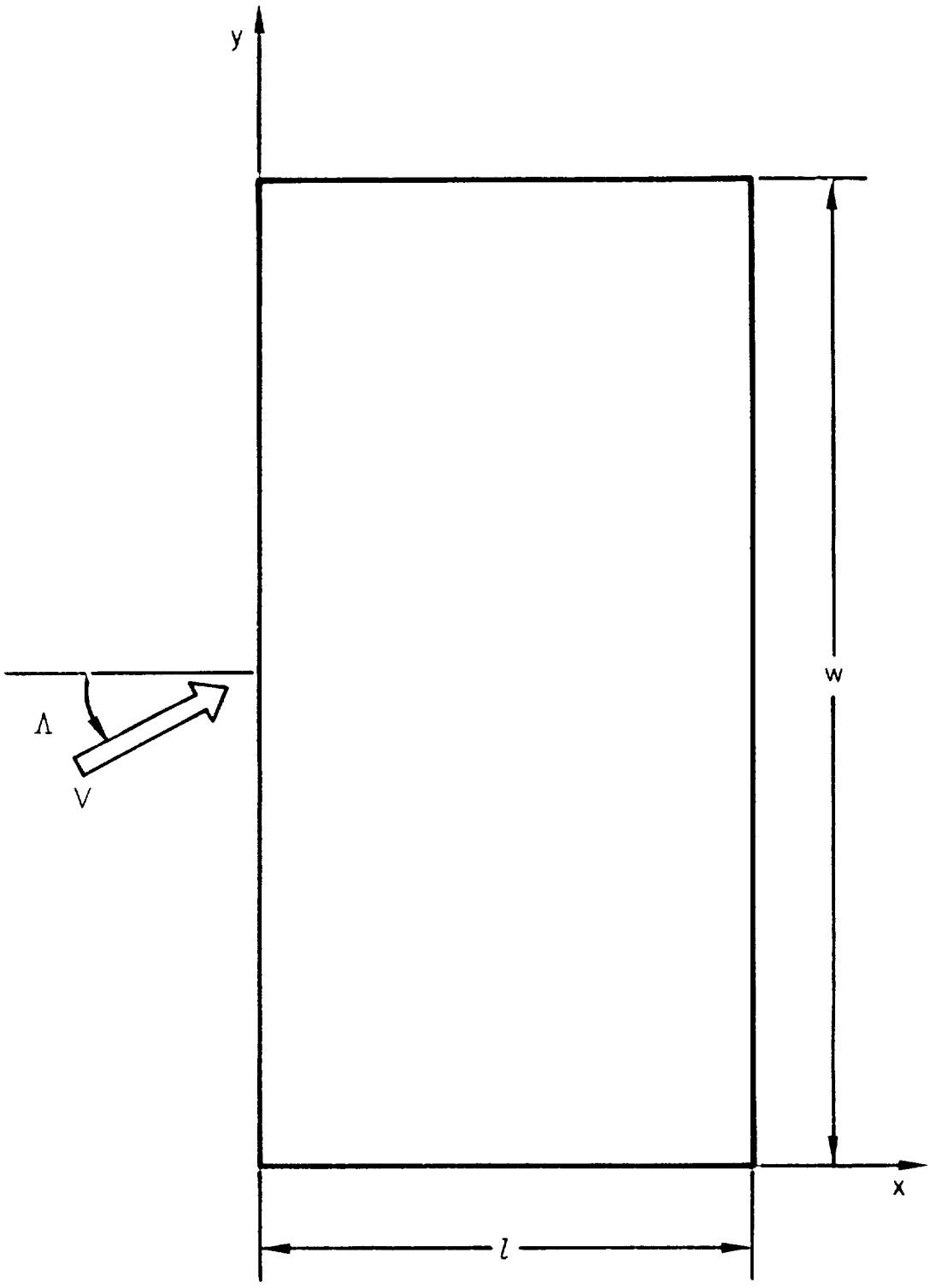

Figure 1.- Panel geometry and coordinate system.

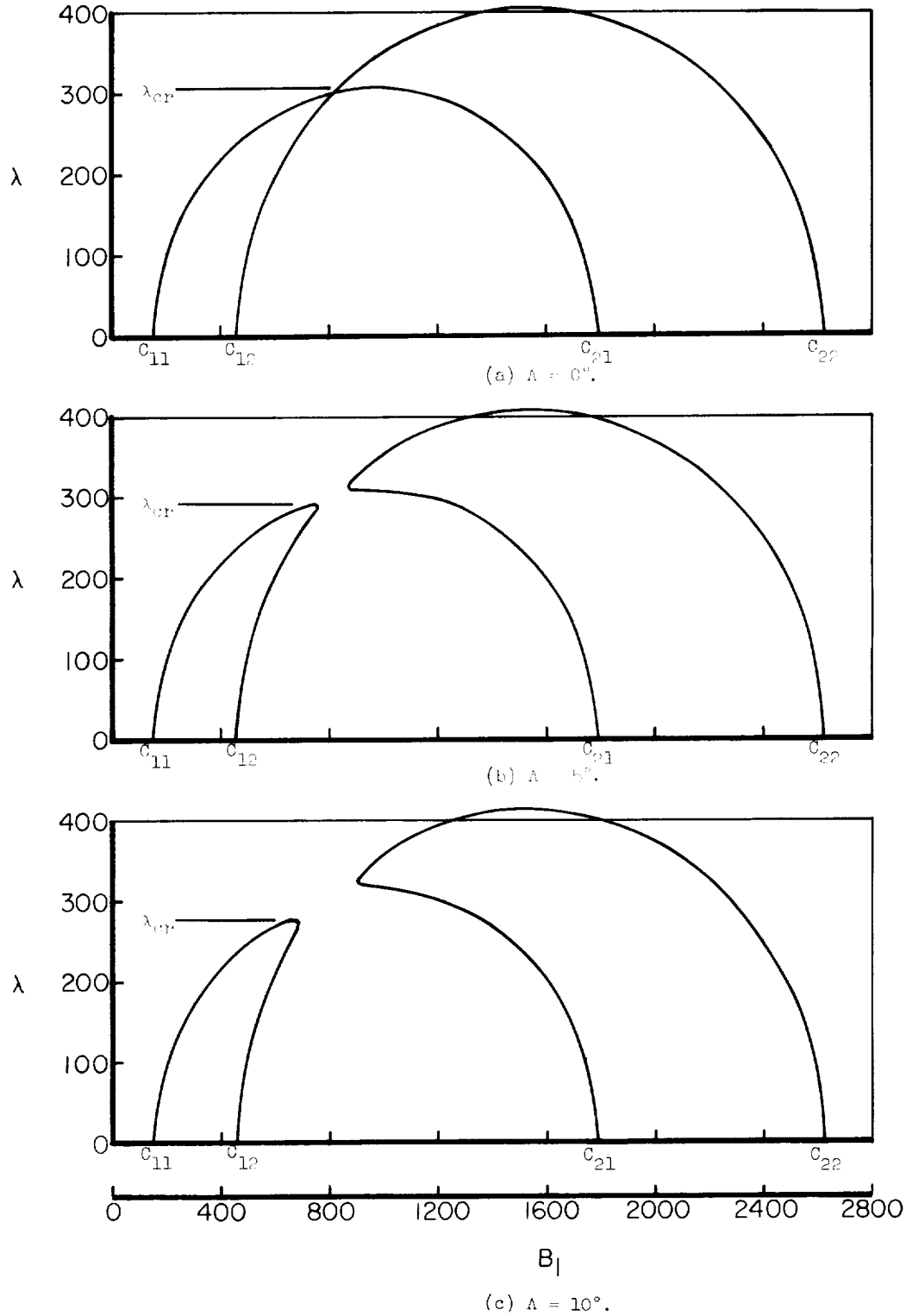

Figure 2.- Variation of dynamic-pressure parameter with frequency parameter. The coefficients C_{mn} are used to indicate the mode associated with the values of the frequency parameter. $\left(\frac{l}{w}\right)^2 = 0.3$.

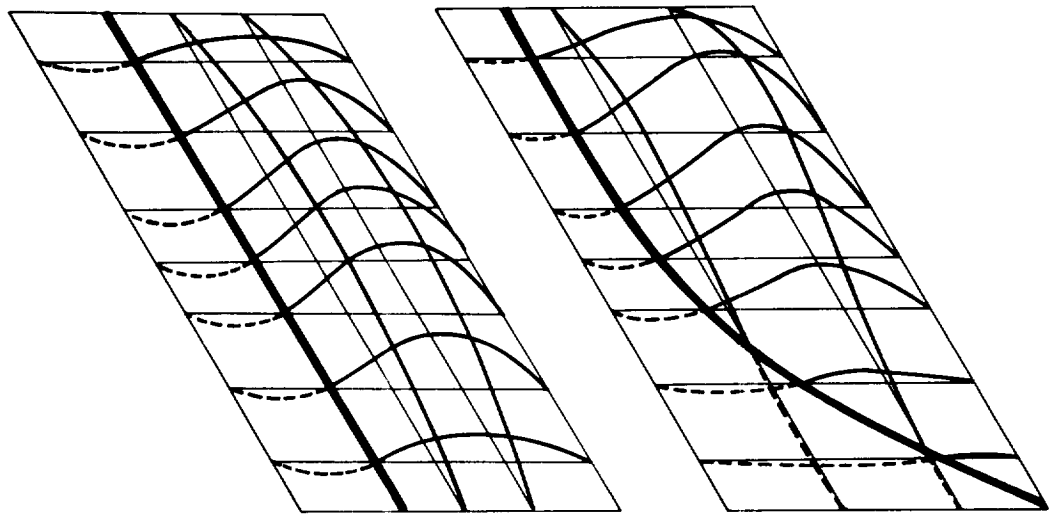

(a) $\Lambda = 0°$.

(b) $\Lambda = 5°$.

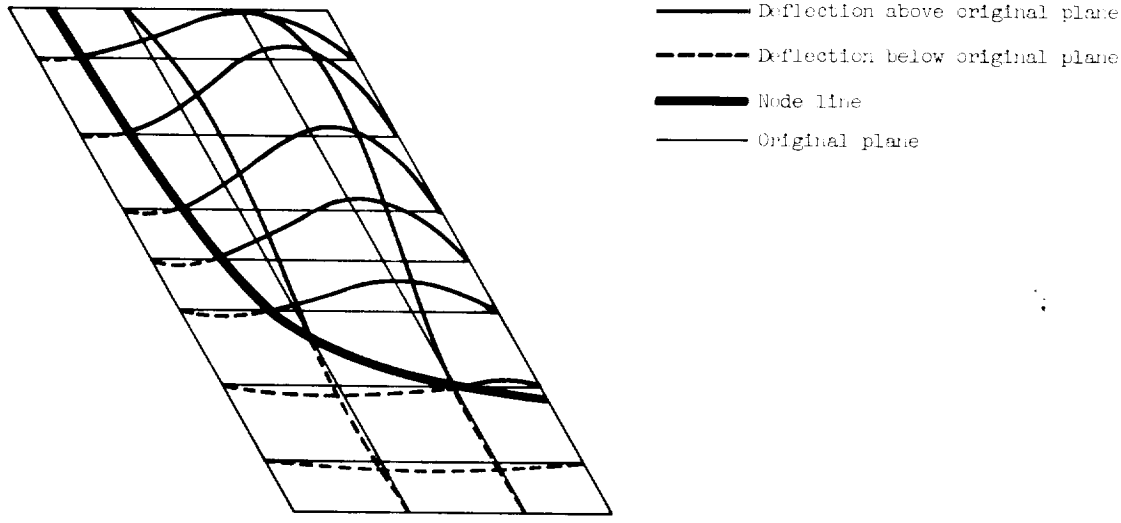

(c) $\Lambda = 10°$.

Figure 3.- Calculated flutter-mode shapes. $\left(\frac{l}{w}\right)^2 = 0.3$.

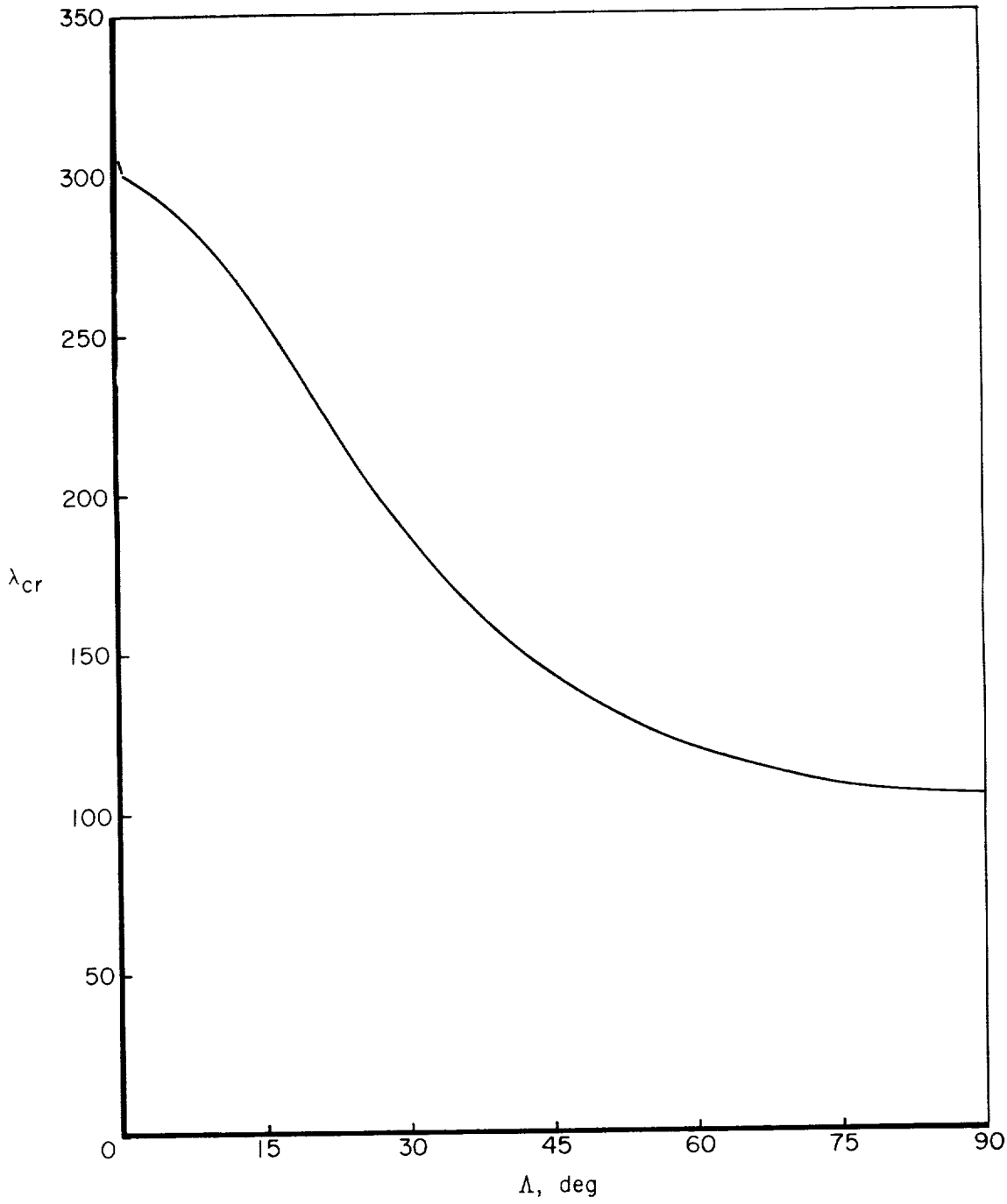

Figure 4.- Variation of critical dynamic-pressure parameter with flow angle. $\left(\frac{l}{w}\right)^2 = 0.3$.

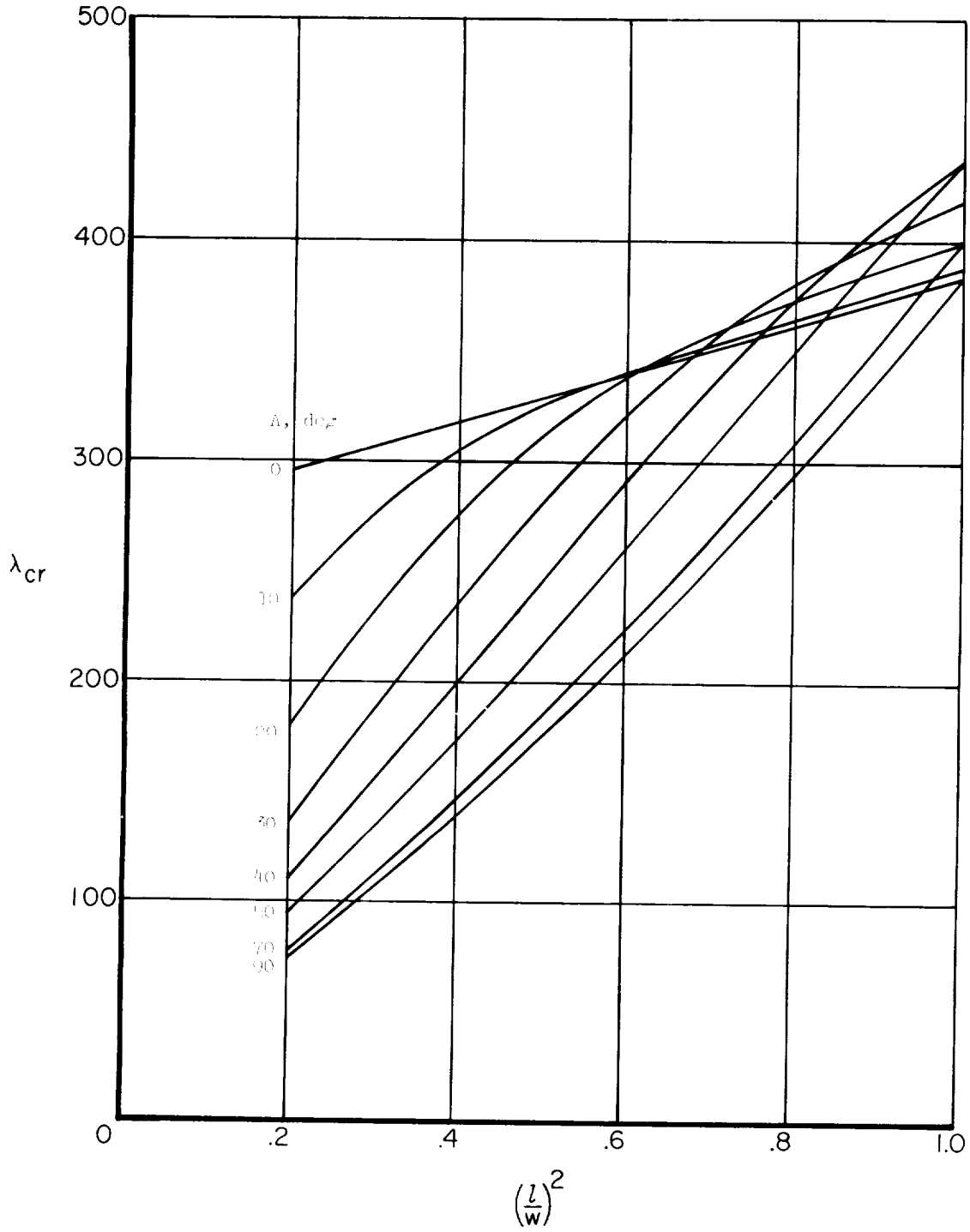

Figure 5.- Effect of length-width ratio on critical dynamic-pressure parameter for various flow angles.

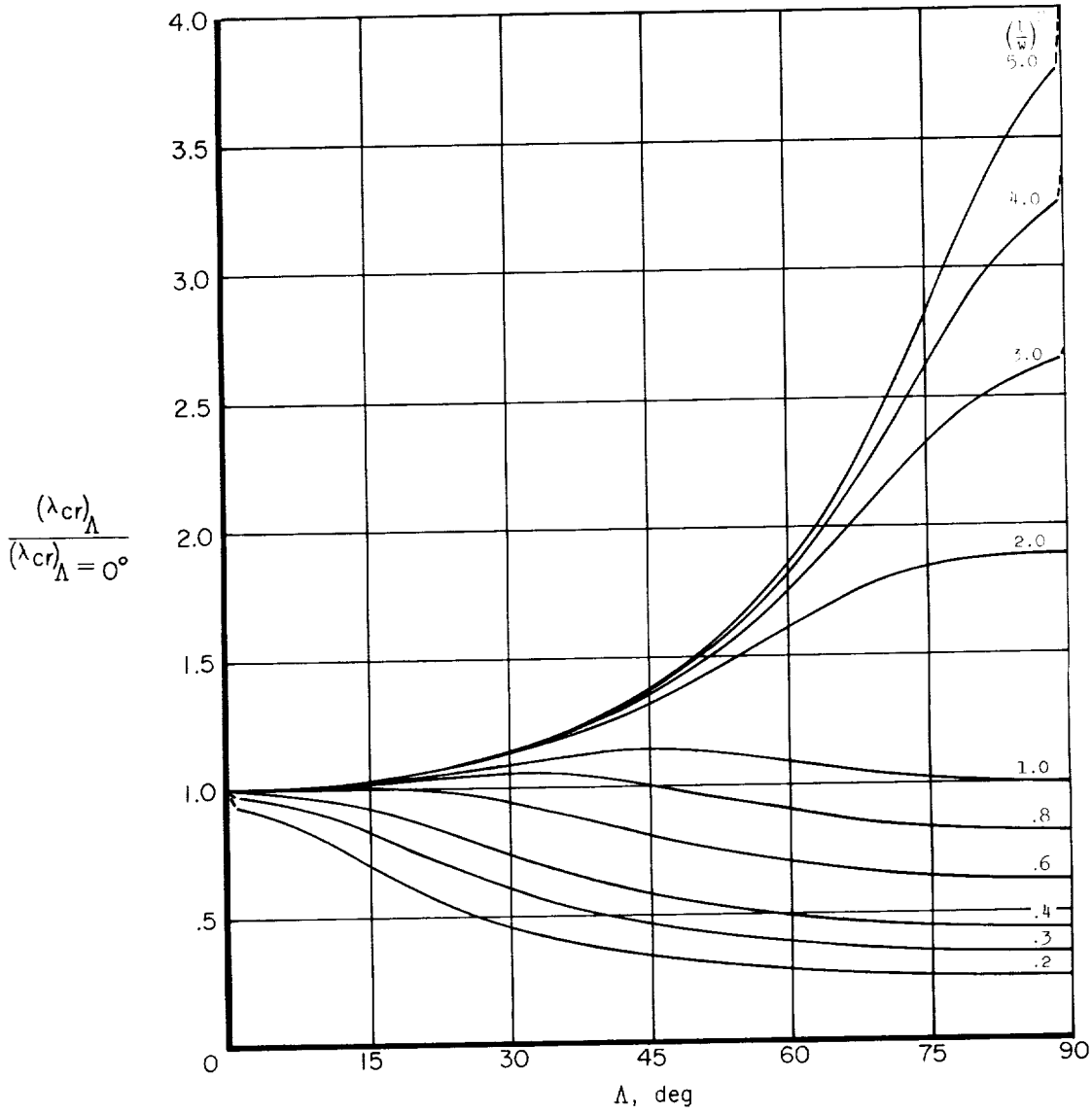

Figure 6.- Effect of flow angle on critical dynamic-pressure parameter for various length-width ratios. Alined panel flow conditions are used as reference.